GRANULAR MICROHYDRODYNAMICS : EMERGENCE OF $f^{-4/3}$ LAW

Hisao Hayakawa
Graduate School of Human and Environmental Studies, Kyoto University, Kyoto 606-01,Japan

Recently granular materials have been studied extensively. Unlike usual solids, liquids or gases, granular materials are known to show fascinating dynamical behaviors [1], such as convection [2], size segregation [3], bubbling [4], standing waves and localized excitations [5,6] under vertical vibration and a fluidized bed due to air injected inside a box containing granules [7,8].

Dynamical behaviors of grains flowing through a vertical pipe which can be regarded as a one dimensional realization of a fluidized bed is also a typical example of unusual features of granular motion [11–15]. Emergence of density waves (slugging) has been investigated by molecular dynamics [9], Stokesian dynamics simulation [10] and lattice-gas automata (LGA) simulations [11,12] and by the experiments using sand or glass beads in air [13,14] and metallic spheres in liquids [15]. In these days, we recognize that the emergence of density waves is closely related to the formation of traffic jams in a highway [16].

Theoretical analysis to understand jam formations has been focused for pure one dimensional cases. Although there are a variety of models such as optimal velocity models [17–19], time delayed models [20] and fluid models [7,8,21,22] to describe such phenomena, we believe that a universal mathematical structure exists which is independent of the choice of models behind these phenomena. From the analysis for pure one dimensional models we have recognized as follows: (i) There is a neutral curve for the linear stability of a uniform flow. (ii) Near the neutral curve, all of models are reduced to the Kortweg deVeries (KdV) equation supplemented by dissipative corrections [8,22–24]. (iii) To describe jam formations, KdV equation is inadequate because its solutions are pulses. (iv) The jam formation is described by an equation at a critical point on the neutral curve where the quadratic term in KdV disappears [18]. (v) We can obtain a steady propagating solution analytically which has asymmetric interfaces to connect dense and dilute regions [18,19]. (vi) Due to the dissipative corrections, the propagating velocity, the width of interfaces and the amplitude have been selected. (vii) The scaled analytic solution near the critical point is very precise near the critical point where its error is less than 1 % [19,25]. The quantitative accuracy of the above statements can be checked from Figs.1 and 2 [19]. Although these are interesting recent progress, we do not pursue the analysis for pure one dimensional models. Readers can see summary of these progresses in Ref. [19,26].

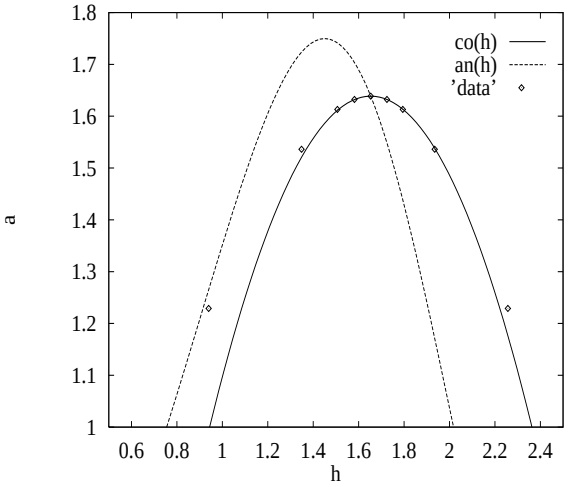

FIG. 1. Theoretical coexistence curve (solid line) $a = a_c(1 - (h - h_c)^2/A^2)$ where $A = 1.13663$, $h_c = 1.65343$ and $a_c = 1.63866$, and the neutral curve (broken line) for the model described by eq.(2) with $W(h) = \tanh(h - 2) + \tanh(2)$, $V(h) = 1 + (1 - \tanh(h - 2))/(1 + \tanh(2))$ and $f_n = 0$. h denotes the average distance between successive cars. The data is obtained for minimum and maximum values of r_n at a given a.[19]

In realistic situations, however, e.g. highways have multi-lanes, and vehicles (particles) can pass slow vehicles (particles). When we include multi-lane effects in one dimensional models, separations between jam and non-jam phases become obscured. However, there is another universal law in quasi one-dimensional systems for dissipative discrete element flows, i.e. a power law in power spectrum of density auto-correlation function of vehicles or particles.

Power-law form of the power spectrum $P(f) \sim f^{-\alpha}$, where f is frequency, of density fluctuations was also found in both numerical simulations [11] and experiments [13,14]. Although their interpretations on the origin of the emergence of density waves are different, estimated values of the exponent α is close to each other ($1.3 < \alpha < 1.5$).

Although the previous experiment [13,14] reported $\alpha \cong 1.5$, some of their experimental procedures seem a little ambiguous: The volume of air flow out of the bottom end of the pipe was not well controlled. Besides, the power spectra they obtained were still noisy. Recently, Moriyama et al. [27] have presented better-controlled air flow out of the pipe and more accurate experimental results than the previous ones by increasing the number of trials [13,14]. One of their results is the precise estimation of the scaling exponent of the power spectrum $P(f) \sim f^{-\alpha}$. The result is $\alpha \cong 1.33$. This result is identical to that by

LGA [11], and is expected to be a universal law in quasi one dimensional dissipative flows such as traffic flows in a highway.

The purpose of this paper is to clarify the mechanism to appear $f^{-4/3}$ law in power spectra. We, thus, extend the one-dimensional model which can be solved without the noise to a stochastic model supplemented by the white noise. We will demonstrate the simple model reproduces $\alpha = 4/3$ near the neutral curve of the linear stability analysis of uniform states.

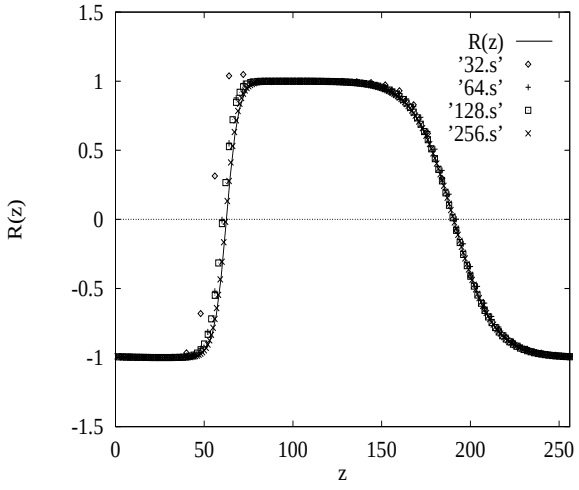

FIG. 2. Theoretical curve (solid line) and scaled data obtained from our simulation for scaled r_n. Each data denotes $(\epsilon, N) = (1/2, 32), (1/4, 64), (1/8, 128), (1/16, 256)$, where $\epsilon = (1 - a/a_c)^{1/2}$, $'N.s'$ represents the data for N cars (particles). Theoretical curve is given by $R(z) = \tanh(\xi\theta_+(z - z_+)) - 1 + \tanh(\xi\theta_-(z - z_-))$ with $\xi = (6\gamma^*)^{1/2}/16$, $\gamma^* = 0.574189$, $\theta_+ = 1.2897187$ and $\theta_- = -0.3876814$, where only $z_+ = 62.5$ and $z_- = 190.5$ are fitting parameters. Spatial scale is measured by the scale for $N = 256$.[19]

Let us introduce a one-dimensional model which reproduces $\alpha = 4/3$. The important mechanisms for particle dynamics are the drag between the air and particles, and the relaxation process to an optimal velocity which may be the sedimentation rate of particles. When the N particles are confined in a quasi-one dimensional container, the motion of particles may be described by the following nonlinear equation:

$$\ddot{r}_n + \zeta[\dot{r}_n - \tilde{W}(\{r_n\})] = TF(\{r_n\}) + f_n(t), \quad (1)$$

where r_n and ζ are the relative distance between the n-th and $n+1$-th particles, and the friction constant, respectively. The collisional force $F(\{r_n\}) = \varphi'(r_{n+1}) + \varphi'(r_{n-1}) - 2\varphi'(r_n)$ comes from a soft core repulsive potential $\varphi(r_n)$. The parameter T represents the strength of repulsion. The optimal velocity $\tilde{W}(\{r_n\}) = U(\frac{r_{n+1}+r_n}{2}) - U(\frac{r_n+r_{n-1}}{2})$ is the linear combination of sedimentation rate $U(r)$ which is the nonlinear function of the local volume fraction [28] in general. The most crucial simplification of (1) is to assume that f_n is a Gaussian white noise with zero mean. It should be noticed that the drag ζ is irrelevant in systems where the bottom end of the pipe is fully open, because air in the pipe flows away together with particles. Thus, to observe density waves it is important to close the cock of the pipe.

We should indicate similarity between our model and a model for traffic flows [19]

$$\ddot{r}_n = a[W(r_{n+1})V(r_n) - W(r_n)V(r_{n-1}) - \dot{r}_n] + f_n, \quad (2)$$

where $W(x)$ and $V(x)$ are respectively monotonic increase and decreasing function of x.

Linearizing (1) around the uniform solution $\dot{r}_n = 0$ where $h = \bar{r}_n \equiv N^{-1}\sum_n r_n$, we obtain

$$\dddot{\tilde{r}}_k + \zeta[\ddot{\tilde{r}}_k - iU'\dot{\tilde{r}}_k \sin k] = 2T\varphi''(\cos k - 1)\dot{\tilde{r}}_k + \dot{\tilde{f}}_k(t), \quad (3)$$

where the argument of U' and φ'' is h. $\tilde{r}_k$ and $\tilde{f}_k(t)$ are respectively the Fourier transform of $\delta r_n = r_n - a$ and $f_n(t)$. Equation (3) has the solution $\tilde{r}_k(t) \propto \exp[\sigma_\pm t]$, where

$$\sigma_\pm = -\frac{\zeta}{2} \pm \sqrt{\left(\frac{\zeta}{2}\right)^2 - 2T\varphi''(1 - \cos k) + i\zeta U' \sin k}. \quad (4)$$

$\mathrm{Re}[\sigma_+]$ represents the relevant eigenvalue of the linear problem, which becomes positive for $U'(h)^2 \cos^2(k/2) \geq T\varphi''(h)$. Thus the most unstable wave number is $k \to 0$ and the neutral curve is given by $T_c = U'^2/\varphi''(h)$. At $T = T_c(1 - \mu)$ the expansion of σ_+ around $k = 0$ is given by

$$\sigma_+(k) \simeq i[c_0 k - \frac{c_0}{6}k^3] + \frac{c_0\mu}{\zeta}k^2 - \frac{c_0^2}{4\zeta}k^4 + \cdots, \quad (5)$$

where $c_0 = U'(h)$. Thus, for $\mu > 0$ the uniform state is unstable due to the negative diffusion.

Adopting $U(r) = \tanh(r - 2) + \tanh(2)$, $\varphi(r) = \mathrm{sech}^2(r)$, $\zeta = 2$, $N = 256$, $T_c = 3.95798\cdots$, and $a = 2$ at $t = 0$, we simulate (1) by the classical Runge-Kutta method until $t = 2^{11}$ with time interval $\Delta t = 1/2^4$ under the periodic boundary condition. We use the uniform random number distributed between $-X$ and X with $X = 9/1024$ for $f_n(t)$. Figure 3 displays the power spectrum $P(f) = |\tilde{c}(f)|^2$ obtained from our simulation of (1) at $\mu = 1/64$, where $\tilde{c}(f)$ is the Fourier transform of the discretely sampled data of the density $c(t) = \dfrac{1}{N}\displaystyle\sum_n \frac{1}{r_n(t)}$ with the interval 1. This clearly supports $P(f) \sim f^{-4/3}$ as in our experiment. It should be noticed that the simulation of (2) also reproduces $P(f) \sim f^{-4/3}$ law. From the examinations of several values of μ, we have confirmed that the qualitative results are insensitive to

the sign of μ when $|\mu| \ll 1$. This result is reasonable because near the neutral curve the time scale of relaxation or growth of fluctuations is much longer than the time scale induced by the noise $f_n(t)$. Our result suggests that the linear relaxation theory of fluctuations can be used to explain $P(f) \sim f^{-4/3}$.

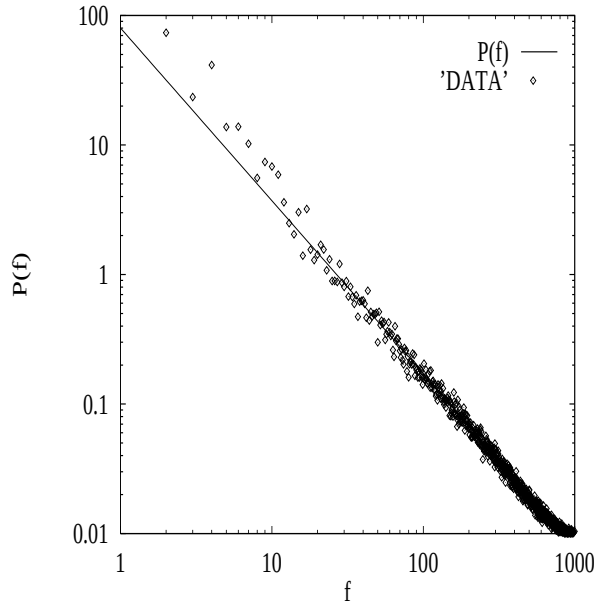

FIG. 3. Log-log plot of power spectrum $P(f)$ obtained from the simulation of (1), where the unit of f is $1/(2\pi)$. The solid line represents $f^{-4/3}$.

Thus, let us briefly explain how to appear $f^{-4/3}$ law from the behavior of structure factor

$$S_k(t) = \sum_{n,m} < \exp[ik(\delta r_n(t) - \delta r_m(0))] > \qquad (6)$$

in weakly stable states, *i.e.*, $\mu < 0$ and $|\mu| \ll 1$. The structure factor can be rewritten as

$$S_k(t) = \frac{1}{N} \sum_{n,m} \exp\left[-\frac{k^2}{2}\phi_{nm}(t)\right], \qquad (7)$$

where $\phi_{nm}(t) =< (\delta r_n(t) - \delta r_m(0))^2 >$. For $\mu < 0$, $S_k(t)$ can be calculated as in the case of polymer dynamics [29]. With the aid of the expansion of σ_+, (1) is reduced to

$$\partial_\tau r(z,\tau) - \partial_z^3 r(z,\tau) = \epsilon[\partial_z^2 - \partial_z^4] r(z,\tau) + \xi(z,\tau), \qquad (8)$$

where $\tau = \epsilon^3 \beta t$, $z = \frac{2\zeta}{3c_0}\epsilon(x + c_0 t)$, $\xi(z,\tau) = \epsilon^3 \beta f_n(t)$ with $\epsilon = \frac{3\sqrt{c_0}}{\zeta}\sqrt{-\mu}$ and $\beta = \frac{4}{3\sqrt{c_0}}$. The solution of (8) is given by $\tilde{r}_k(\tau) \simeq \int_0^\tau ds \exp[\lambda_k(\tau - s)]\tilde{\xi}_k(s)$, where $\lambda_k = ik^3 - \epsilon k^2(1 + k^2)$. Thus, we obtain the correlation

$$< \tilde{r}_k(\tau)\tilde{r}_{-k}(0) >= \frac{D}{2\epsilon l k^2(1+k^2)} \exp[\lambda_k \tau], \qquad (9)$$

where l is the system size, and we use $< \tilde{\xi}_k(\tau)\tilde{\xi}_p(\tau') >= \frac{D}{l}\delta_{k+p,0}\delta(\tau - \tau')$.

The procedure to obtain the structure factor is parallel to that for polymer dynamics [29]. Substituting (9) into $\phi(z,z',t) =< (r(z,t) - r(z',t))^2 >$ which is the continuous limit of the scaled ϕ_{nm}, we obtain

$$\phi(z,z',t) = 2D_G t + \frac{D}{2\epsilon l}\sum_{n\neq 0} \frac{1}{k^2(1+k^2)} \times \left\{ |e^{ikz} - e^{ikz'}|^2 + 2(1 - e^{\lambda_n t})e^{ik(z-z')} \right\} \qquad (10)$$

With the aid of $\sum_{n\neq 0} \frac{1}{k^2(1+k^2)} \simeq \frac{l^2}{3} - l$ and $\sum_{n\neq 0} \frac{\cos(k(z-z'))}{k^2(1+k^2)} \simeq \frac{l^2}{3} - l|z - z'|$, the first term of (10) is reduced to

$$\sum_{n\neq 0} \frac{|e^{ikz} - e^{ikz'}|^2}{k^2(1+k^2)} \simeq 2l|z - z'|. \qquad (11)$$

On the other hand, the second term of (10) becomes

$$\sum_{n\neq 0} \frac{e^{ik(z-z')}}{k^2(1+k^2)}(1 - e^{\lambda_n t}) = 2\sum_{n=1}^{\infty} \frac{\cos[k(z-z')]}{k^2(1+k^2)} \times \{1 - \cos(k^3 t)\} + 2\sum_{n=1}^{\infty} \frac{\sin[k(z-z')]}{k^2(1+k^2)} \sin(k^3 t). \qquad (12)$$

Replacing the summation $\sum_{n=1}^{\infty}$ to the integral $\int_0^\infty dk$, and substituting (10)-(12) into (7), we obtain

$$S_k(\tau) \simeq \int_{-l}^{l} dx \exp[-D_G k^2 \tau - \frac{Dk^2}{2\epsilon} w - \frac{Dk^2}{\pi\epsilon}\tau^{1/3} h(u)], \qquad (13)$$

where $w = |z - z'|$, $u = x\tau^{-1/3}$, and the argument of S_k is replaced by the scaled time. D_G is the diffusion constant for the gravitational center in (8), and $h(u)$ is

$$h(u) = \int_0^\infty dQ[\frac{\cos(Qu)}{Q^2(1 + \tau^{-2/3}Q^2)}(1 - \cos(Q^3)) + \frac{\sin(Qu)\sin(Q^3)}{Q^2(1 + t^{-2/3}Q^2)}], \qquad (14)$$

where $Q^3 = k^3\tau$, and $w = |z - z'|$. Since $h(u)$ converges to $h(0) = \pi/\Gamma(1/3)$ as time goes on, we obtain

$$S_k(\tau) \simeq \frac{\epsilon}{Dk^2} \exp[-\frac{Dk^2}{\epsilon\Gamma(1/3)}\tau^{1/3}] \qquad (15)$$

in intermediate time range. In the limit of small τ, $S_k(\tau) \propto 1 - \frac{Dk^2}{\epsilon\Gamma(1/3)}k^2\tau^{1/3} + \cdots$. Thus its Fourier transform, which is nothing but the power spectrum $P_k(f) = |\tilde{c}_k(f)|^2$ obeys

$$P_k(f) \sim f^{-\alpha}, \quad \alpha = 4/3 \quad (\text{as} \quad f \to \infty), \qquad (16)$$

where use was made of $\int_{-\infty}^{\infty} d\tau e^{i2\pi f\tau}|\tau|^{1/3} \propto f^{-4/3}$. The value 4/3 is identical to the one obtained by the experiment [27] and numerical simulations [11,27]. Thus our model (1) reproduces $\alpha = 4/3$. This result should be valid even when we start from fluid models [8,21] since the result is determined by the universal feature near the neutral curve. It should be noted that the appearance of this power-law form in the original model (1) is only for $f < \zeta$ since we eliminate the fast decaying mode σ_- in our analysis. This tendency is also observed as the higher-frequency cutoff in the experiment [27].

Thus, $f^{-4/3}$ law is determined by short time behavior of the dynamics of density waves induced by the noise, which is essentially determined by the linear dispersion relation $\lambda_k \sim ik^3$.

In this paper we have confirmed the universal law of $\alpha = 4/3$ as the power-law exponent in the frequency spectrum of density correlation function from the simulation and the theory. We have also clarified the mechanism to emerge $f^{-4/3}$ spectrum which is related to the critical slowing down of the density fluctuations. It should be noticed that the continuous increase of α in LGA [12] from $\alpha = 0$ to 2 with the particle density is consistent with 4/3 law and our picture, because the spectrum determined by the noise in linearly stable uniform state far from the neutral curve should be white ($\alpha = 0$) and the effective exponent of the power-law becomes large when the exponential decay (i.e. $\alpha = 2$) in the off-critical region exists. There is, however, discrepancy between our results with the one on the experiment in liquids [15]. The reason of this difference should be clarified in the future.

The author thanks O. Moriyama, S.Wada and K. Nakanishi for fruitful discussions. This work is partially supported by Grant-in-Aid for Science Research Fund from the Ministry of Education, Science and Culture (09740314).

[1] H. M. Jaeger, S. R. Nagel and R. P. Behringer, Rev. Mod. Phys. **68**, 1259 (1996).
[2] Y-h. Taguchi, Phys. Rev. Lett. **69**, 1367 (1992), K. M. Aoki T. Akiyama, Y. Maki and T. Watanabe, Phys. Rev. E **54**, 874 (1996).
[3] A. Rosato, K. J. Strandburg, F. Prinz and R. H. Swendsen, Phys. Rev. Lett. **58**, 1038 (1987).
[4] H. K. Pak and R. P. Behringer, Nature **371**, 231 (1994).
[5] F. Melo, P. B. Umbanhowar and H. L. Swinney, Phys. Rev. Lett. **75**, 3838 (1995).
[6] P. B. Umbanhowar, F. Melo and H. L. Swinney, Nature **382**, 793 (1996).
[7] G. K. Batchelor, J. Fluid Mech. **193**, 75 (1988).
[8] S. Sasa and H. Hayakawa, Europhys. Lett. **17**, 685 (1992), T. S. Komatsu and H. Hayakawa, Phys. Lett. A **183**, 56 (1993).
[9] J. Lee, Phys. Rev. E **49**, 281 (1994).
[10] K.Ichiki and H. Hayakawa, Phys. Rev. E **52**, 658 (1995).
[11] G. Peng and H. J. Herrmann, Phys. Rev. E **49**, R1796 (1994).
[12] G. Peng and H. J. Herrmann, Phys. Rev. E **51**, 1745 (1995).
[13] S. Horikawa, A. Nakahara, T. Nakayama and M. Matsushita, J. Phys. Soc. Japan **64** 1870 (1995).
[14] S. Horikawa, T. Isoda, T. Nakayama, A. Nakahara and M. Matsushita, Physica A **233**, 699 (1996).
[15] A. Nakahara and T. Isoda, Phys. Rev. E **55**, 4264 (1997).
[16] e.g. G.B.Whitham, Linear and Nonlinear Waves (Wiley, New York, 1974); R. Huberman, Mathematical model: Traffic flow (Prentice Hall, 1977); D.Helbing, Traffic Dynamics: New Physical Modeling Concepts (Springer, Berlin, 1997).
[17] M. Bando, K. Hasebe, A. Nakayama, A. Shibata and Y. Sugiyama, Phys. Rev. E **51**, 1035 (1995).
[18] T. S. Komatsu and S. Sasa, Phys. Rev. E **52**, 5574 (1995).
[19] H. Hayakawa and K. Nakanishi,patt-sol/9707002.
[20] L.A.Pipes, J.Appl.Phys. **24**, 274 (1953): G.F. Newell, J.Oper.Res. Soc.Am. **9**, 209 (1961): D.C. Gazis, E.Herman, and R.W. Rothery, J.Oper.Res.Soc. Am **9**, 545 (1961).
[21] B. S. Kerner and P. Konhauser, Phys. Rev. E **48**, 2335 (1993).
[22] D. A. Kurtze and D. C. Hong, Phys. Rev. E **52**, 218 (1995).
[23] M. F. Göz, Phys.Rev.E **52**,3697 (1995).
[24] G.B. Whitham, Proc. Roy. Soc. Lond. A **428**, 49 (1990).
[25] S.Wada and H.Hayakawa, in preparation.
[26] H. Hayakawa and K. Nakanishi, Prog. Theor. Phys. Suppl. (to be published).
[27] O.Moriyama, N.Kuroiwa, and M.Matsushita, and H.Hayakawa, preprint.
[28] H.Hayakawa and K.Ichiki, Phys.Rev. E **51**, R3815 (1995) and references therein.
[29] P.G. de Gennes, Physics **3**, 37 (1967): M. Doi and S. F. Edwards, *The Theory of Polymer Dynamics* (Oxford, 1986).